CHAPTER II
LITERATURE REVIEW

2.1 Conductive Polymers

An organic polymer that possesses the electrical, electronic, magnetic, optical properties, and meanwhile retaining the mechanical properties, processibility of the conventional polymer is termed an 'intrinsically conducting polymer' (ICP), more commonly known as a 'synthetic metal'. For the past 50 years, conventional insulating polymer system have been increasingly used as substitutes for structural materials such as wood, ceramic, and metals because of their light weight, high strength, ease of chemical modification/customization, and processibility at low temperature. In 1977, the first electrically conducting organic polymer, doped polyacetylene, was reported, spurring interest in 'conducting polymer'. The common electronic feature of pristine (undoped) conducting polymeris a π-conjugated system which is form by the overlap of carbon p_z orbital and alternating carbon-carbon bond lengths shown in schematically in Figure 2.1. Other conducting polymers found are, for examples, poly(p-phenylene) (PPP), polypyrrole (PPy), poly(p-phenylene)sulphide (PPS), polythiophene (PTh), polycarbazole (PCB), polyquinoline, and polyaniline (PANI)

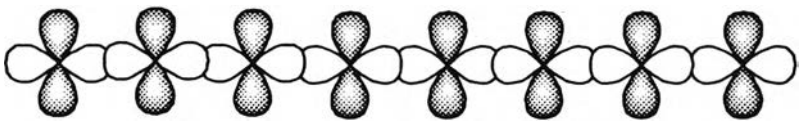

Figure 2.1 The π-conjugated system in the polyacetylene.

2.1.1 Conduction Mechanisms

Electrical conductivity is as function of the number of charge carriers of species 'i' (n_i), the charge on each carrier (ε_i), and carrier mobilities (μ_i). Conduction in solids is usually explained in the terms of the band theory which is described by the relation $\sigma = \sum \mu_i n_i \varepsilon_i$ where the unit of conductivity is S cm^{-1}. It is postulated that

when atoms or molecules are formed in the solid state, the outer atomic orbitals containing the valence electrons are split into bonding and antibonding orbitals, and are mixed to form two series of closely-space energy level. These are usually called the valence band and conduction band, respectively. If the valence band is only partly filled by available electrons, or if the two bands overlab so that no energy gab exists between them, then the application of an electrical potential will raise some of electrons into empty levels where they will be free to move throughout the solid thereby producing a current. This is the description of a *conductor.* If, on the other hand, the valence band is full and is separated from the empty conduction band by an energy gap, then there can be no net flow of the electrons under the influence of an external field unless the electron are elevated into the empty band and this process will require a considerable expenditure of energy. Such materials are either semiconductors or insulators, depending on how large energy gap may be. The band model then assumes that the electrons are delocalized and can extend over the lattice. The majority of polymers are insulator.

For the electrical conduction in a polymer, the band theory is not totally suitable because the atoms are covalently bonds to another one, forming polymeric chains that experience weak intermolecular interactions. Thus macroscopic conduction will require electron movements, not only along chains but also from one chain to another.

2.1.2 The Concept of Doping

Doping process describe as the method for achieving the high electrical conductivity. The doping of all conductive polymers is accomplished by the redox doping. This involves the partially addition (reduction) or removal (oxidation) of electrons to or from the π-system of the polymer backbone.

The concept of doping is of a unique underlying theme which distinguishes conductive polymers from all other types of polymers. During the doping process, an organic polymer, either an insulator or semiconductor, having a small conductivity, typically in the range 10^{-10} to 10^{-5} S cm^{-1}, is converted to the polymer which residues in the 'metallic' conducting regime (ca. 1 to 10^{4} S cm^{-1}). The

controlled addition of known, usually small (< 10%) and non-stoichiometric quantities of chemical species results in dramatic change in electronic, electrical, magnetic, optical, and structural properties of the polymer. Doping can be reversible to produce the original polymer with a little or no degradation of the polymer backbone. Doping and undoping processes, involving dopant counterions which stabilize the doped state may be carried out chemically or electrochemically.

In the 'dope state', the polymer backbone of conductive polymer consist of a delocalized π-system. In the 'undoped state', the polymer may have a conjugated backbone such as in trans-$(CH)_x$ or it may have a non-conjugated backbone, as in polyaniline (leucoemeradine base form), which becomes conjugated only after doping or a non-conjugated structure as in the emeraldine base form of polyaniline which becomes conjugated only after protonic acid doping.

2.1.3 Doping Process

Doping process can be divided into three main types:

2.1.3.1 Redox Doping involving Dopant Ions

All conductive polymer (and most of their derivatives), e.g.

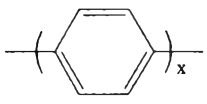

Poly(p-phenylene)

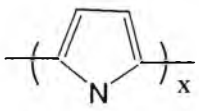

Polypyrrole

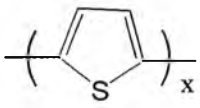

Polythiophene

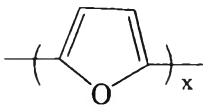

Polyfuran

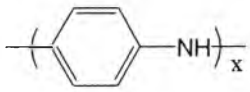

Polyaniline

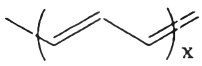

Polyacetylene

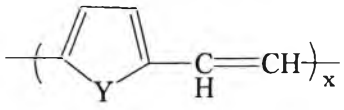

Poly(heteroaromatic vinylenes)

(where Y = NH, NR, S, and O); etc, undergo either *p*- and/or *n*-redox doping by chemical and/or electrochemical processes during which the number of electrons associated with the polymer backbone changes.

2.1.3.1.1 Chemical and Electrochemical p-Doping

p-doping, partial oxidation of the π-system of an organic polymer, was first discovered by treating *trans*-polyacetylene with an oxidizing agent such as iodine viz.

$$trans\text{-}[CH]_x + 1.5\,xy\,I_2 \longrightarrow [CH^{+y}(I^3)^-_y]_x \qquad (y < 0.07)$$

This process was accompanied by increase in conductivity from ca. 10^{-5} to 10^3 S cm^{-1}.

2.1.3.1.2 Chemical and Electrochemical n-Doping

n-doping, partially reduction of the π-system of an organic polymer, was also discovered by using *trans*-polyacetylene and treating it with an reducing agent such as liquid sodium amalgam or preferable sodium naphthalide, viz.

$$trans\text{-}[CH]_x + (xy)Na^+ (Naphth)^- \longrightarrow [Na_y^+ CH^{-y}]_x + Naphth \qquad (y < 0.1)$$

The antibonding π* system is partially populated by this process which is accompanied by an increase in conductivity of ca. 10^3 S cm^{-1}.

2.1.3.2 Redox Doping involving No Dopant Ions

2.1.3.2.1 Photo-doping

When *trans*-polyacetylene, for example, is exposed to a radiation of energy greater than its band gap electrons are protonated across the gap and the polymer undergoes 'photo-doping'.

2.1.3.2.2 Charge-injection Doping

It is the most conveniently carried out using a metal/insulator/semiconductor (MIS) configuration involving a metal and a conductive polymer separated by a thin layer of a high dielectric strength insulator. Application of an approxpriate potential across the structure can give rise, for example, to a surface charge layer, the 'accumulation' layer which has been extensively investigated for conductive polymer. The resulting charges in the polymer, e.g. $(CH)_x$ or poly (3-hexylthinylene) are present without any associated dopant ions so that the spectroscopic properties of the charged species so formed can be examined in the absence of dopant ions. However, the coulombic interaction between charges

on the chain and dopant ions is a very strong interaction and one that can totally alter the energetic of the system. Studies of this type of polymers strongly suggest that the formation and role of bipolarons in the chemically and/or electrochemically doped polymers should be carefully re-examined since they may be stable only in the presence of the dopant counterion.

2.1.3.3 Non-redox Doping

This type of doping process differs from the redox doping descried above in that the number of electrons associated with the polymer backbone does not change during the doping process. It is accomplished by treating an emeraldine base with aqueous protonic acids and it accomplished by nine to ten order of magnitude increase in conductivity (up to ca. 10^2 S cm^{-1}) to produce the protonated emeraldine base, viz.

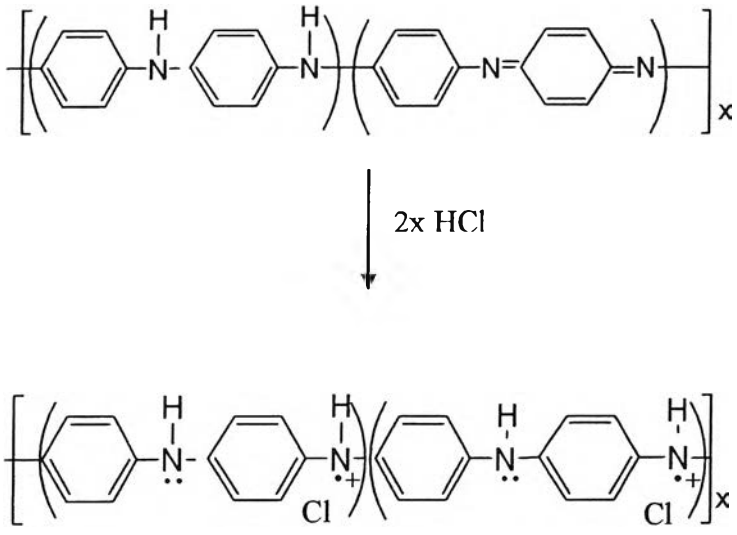

Scheme 2.1 Doping process of emeraldine base polyaniline by protonic acids.

2.1.4 Literature Reviews of Conductive Polymers

Lee *et al.* synthesized polythiophene nanowires by using gamma radiation induced oxidative chemical polymerization. They reported that the flower-liked morphology with diameter around 50-100 nm and a length is up to several millimetre were obtained. Different characterization methods including elemental analysis, FTIR, Raman spectroscopy, and X-ray photoelectron microscopy were

utilized to prove that the conducting polythiophene was successfully synthesized by this facile method.

Demoustier-Champa *et al.* synthesized polypyrrole nanotubules by using chemical and electrochemical polymerizations of pyrrole monomer in the presence of the nanoporous polycarbonate acting as a template. Field-Effect Scanning Electron Microscope (FE-SEM) was used to investigate the morphology of the synthesized products. Form the result; it was found that both electrochemical and chemical methods could produce the polypyrrole nanotubules. However, the prefectly cylindrical 15 nm polypyrrole was obtained by chemical synthesis.

Lupshak *et al.* prepared the uniform layer of polyparaphenylene (PPP) on Pt, graphite electrod by using anodic polymerization of benzene in sulfonic acid and in the presence of sodium alkyl sulfonate as a surfactant. Cyclic voltammetric curves in the inorganic and organic media showed that the rate of charge-transport processes and the redox stability of PPP films depended on nucleophilic agents and electron donor properties of of solvents. Moreover, the reversible electrochemical behavior was observed in sulfuric acid solution and in organic solvent with donor number $DN \leq 15$.

Shirakawa synthesized polyacetylene by using an interfacial polymerization of acetylene monomer on a surface of a concentrated homogeneous Ziegler-Natta catalyst solution. Thin film products were obtained and subjected to characterize various properties. The author also reported that the quality of the films was dependent strongly on method used to prepare the catalyst as well as the polymerization conditions of acetylene.

Hosseini and Entezami synthesized various N-(carbohydroxamic acid) pyrrole and N-(carbohydroxamic acid) carbazole derivatives by chemically and electrochemically polymerization in a specific condition. The electrical conductivity of the synthesized products was measured by four probe method. Moreover, it was further reported that the synthesized products gave coloured complexes with certain metals.

2.2 Polyaniline

2.2.1 General Background

Polyaniline is one of the conductive polymers synthesized by chemical oxidation or by electrochemically polymerization in the presence of acid media. Polyaniline has a general formula containing reduced repeat units, and oxidized repeat units. The general formula of polyaniline is shown in the Scheme 2.2.

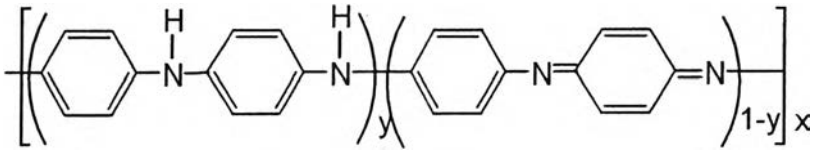

reduced repeat units oxidized repeat units

Scheme 2.2 The general formula of polyaniline.

Polyaniline can exist in three different oxidation states with different colours. The fully reduced form of polyaniline, Leucoemeraldine, corresponds to a value of y = 1; the fully oxidized form of polyaniline, Pernigraniline, corresponds to a value of y = 0; and the half oxidation form of polyaniline, Emeraldine, corresponds to a value eof y = 0.5. The different oxidation states of polyaniline are shown in the Scheme 2.3.

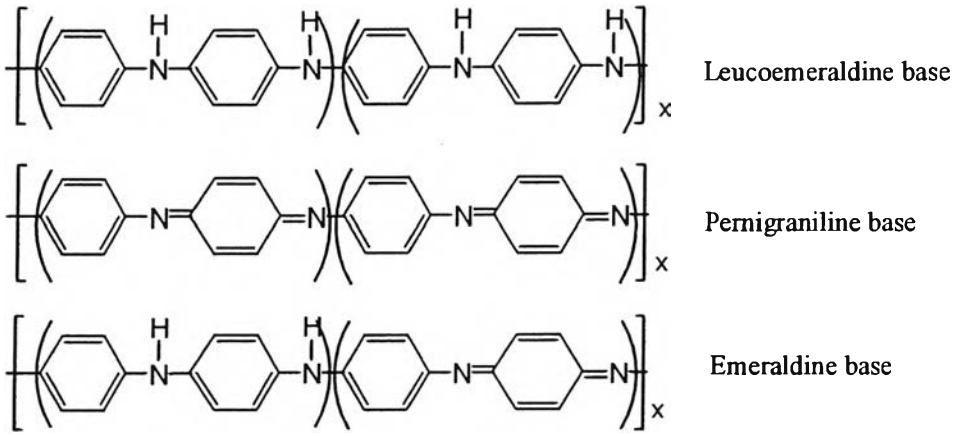

Scheme 2.3 The different oxidation states of polyaniline.

Each oxidation state can exist in the form of its base or its protonated form (salt) by treatment with an acid. The different oxidation states of polyaniline can interconverse process of polyaniline is shown in Scheme 2.4.

The insulating emeraldine base form of polyaniline can be converted to the conducting emeraldine salt form by two independent doping methods:

1) Oxidation doping method by chemical reaction with an appropriate oxidizing agent such as $FeCl_3$ and electrochemical charge transfer reaction. The charge transfer reaction causes a change in the total number of π-electron on the conjugate chain.

2) Protonation doping with acid-base reaction in the aqueous media with pH less than 2-3. There is no change in the number of π-electron.

In the recent years, polyaniline (PANI) has been considered as one of the most potential conducting polymers for various electrochemical, electrorheological and electronic applications such as batteries, sensors, controlling systems and organic displays because of its facile synthetic process, good environmental stability, easy conductivity control and cheap production in large quantities. However, its processability to make either films or coated layers is rather difficult because it is infusible and insoluble in common solvents and the product from pure polyaniline shows low mechanical properties, therefore, the above-mentioned commercial applications have been limited.

The general method used to solve these problems is to fabricate the polymer composite or polymer blend with other polymer matrix. The polymer composite of conductive polymer and other polymer matrix can enhance the processibility and mechanical properties of the conductive polymer while the inherent properties of conductive polymer are still retained

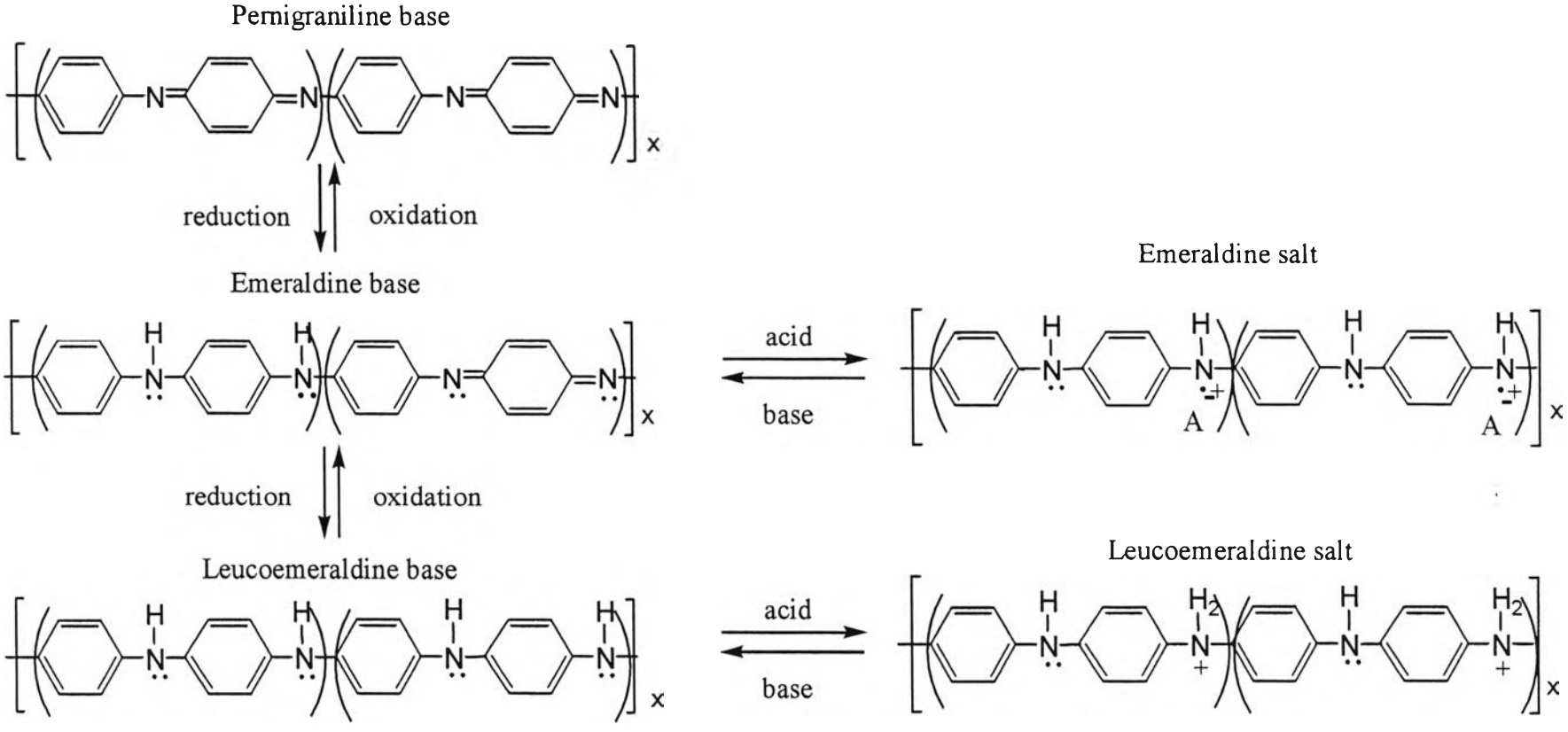

Scheme 2.4 A reaction diagram consistent with the interconversion of different oxidation and protonation states of polyaniline.

2.2.2 Literature Reviews of Polyaniline

The emeraldine salt form of polyaniline was synthesized electrochemically as a film exhibiting a well defined fibrillar morphology closely resembling that of polyacetylene by Huang *et al.* (1986). It was proposed that the emeridine form of polyaniline had the symmetrical conjugation structure having extensive charge delocalization resulting from a new type of doping of an organic polymer-salt formation rather than oxidation which occurred in the *p*-doping of all other conducting polymer systems.

Cao *et al.* (1989) studied the relationships between the chemical polymerization conditions and the physicochemical properties of polyaniline. The results showed that the reaction yield was not strongly sensitive to most synthesis variables, while the viscosity, or molecular weight, and the electrical conductivity of the as-polymerized and/or post-treated polyaniline salt were found to be markedly affected.

Stejskal and Kratochvil (1996) studied the oxidative polymerization of aniline. The results indicated that the variety forms of polyaniline have different conductivity and colour.

The chemical polymerization of aniline was carried out in media containing different linear dicarboxylic acids with the use of oxidants such as $K_2Cr_2O_7$, $KMnO_4$, $K_2S_2O_8$, KIO_3 and $FeCl_3$ (Erdem *et al.* 2004). The results showed that among the oxidants employed the best result was obtained with $K_2Cr_2O_7$. Furthermore, it was not observed a remarkable change in the conductivities of polyaniline samples in air within the period of 50 days. Doped polyaniline were partly soluble in organic solvents such as DMF, DMSO and NMP. The intrinsic viscosity and density values of polyaniline samples were observed to decrease as the dopant anion becomes larger.

2.3 Polyaniline Nanostructures

Intrinsically conducting polymers, including polyacetylene, polyaniline (PANI), polypyrrole, polythiophene, poly (*p*-phenylene-vinylene), etc., are termed

organic polymers that possess the electrical, electronic, magnetic, and optical properties of a metal while retaining the mechanical property, processability, etc. commonly associated with a conventional polymer, and more commonly known as "synthetic metals". Of these polymers, PANI has elicited the most interest since its electrical conductivity was found by (MacDiarmid, Chiang, Halpern, Mu, Somasiri, Wu, Yaniger 1985) due to its wide range of conductivity from insulating to metallic regime, unique redox tunability, good environmental stability, low cost, ease of synthesis, and promising applications in various fields, such as metallic corrosion protection, electromagnetic interference shielding, electrostatic discharge, sensors, actuators, to mention just a few. PANI and its derivatives are generally synthesized by chemical or electrochemical oxidative polymerization of the monomers, although some other approaches such as plasma polymerization, electroless polymerization, and solid-state polymerization were also reported. Note that the intractability, i.e., infusibility and insolubility, is the main factor that hampers the applications of PANI, dispersing of the polymer in conventional polymers was considered one of the most effective approaches to address this problem from both the scientific and technological point of view. Accordingly, synthesis of nano-structured PANI, on one hand, is the key step in preparing highly dispersed blend of PANI with other processable polymers, and thus to improve the processability of PANI. On the other hand, some special physical and chemical properties differing from the bulk material will be achieved on nano-structured PANI and will render it for new applications, such as chemical sensors, energy conversion and storage, light-emitting display devices, microelectronics, optical storage, and so on. In comparison with the PANI nanoparticles, which are mainly synthesized by dispersion technique and electrochemical method and have been the subject of a recent review (Behera, Bag, Alam, Mathur 2004), one dimensional nano-structured PANI, including nanofibers, nanowires, nanorods, nanotubes, nanofibrils, nanobelts and nanoribbons, presents several advantages in fabricating nano-devices and in preparing nanoscale electrical connections in highly conducting polymer composites, etc. The objective of this paper is to review the past works concerning the synthesis and applications of one-dimensional nano-structured PANI. It should be emphasized that the paper is only

intended to provide a brief summary of the literature and omissions are inevitable due to the myriad of investigations carried out on this subject.

Aside from the physical routes like electrospinning and mechanical stretching, and the doping induced solution route, the chemical approaches adopted for production of one-dimensional nano-structured PANI can be generally categorized into the chemical oxidative way and the electrochemical oxidative way, just as that occurred for the synthesis of the conventional PANI powders. While in this review, the synthesizing approaches used for production of one-dimensional nano-structured PANI, as detailed below, are divided into two categories, i.e. the template synthesis and the no-template synthesis, in the light of whether template(s) is (are) used or not. The former is subdivided into hard template (physical template) synthesis and soft template (chemical template) synthesis approach according to the solubility of the templates in the reacting media, while the latter is subdivided into interfacial polymerization, radiolytic synthesis, rapid mixing reaction method and sonochemical synthesis. Other approaches like seeding polymerization and combined soft and hard template synthesis were also reported.

2.3.1 Synthesis of Polyaniline Nanostructures

2.3.1.1 Template Synthesis

2.3.1.1.1 Hard Template Synthesis

The hard template synthesis method, which is proposed by Martin *et al.* (Martin 1994; 1996; 1996), involves synthesizing the intrinsically conducting polymers like PANI, polypyrrole, as well as other materials including metals, carbons, in the pores, channels of hard templates such as membranes, zeolites, anodic aluminum oxide (AAO), and so on. One of the interesting and useful features of the method is its effectiveness in preparing one-dimensional micro- or nano-structured materials with controllable diameter, length and orientation. For example, PANI filaments with diameters of 3 nm have been achieved in the hexagonal channels of mesoporous aluminosilicate. However, the disadvantage of the method is that, firstly, a rather tedious post-synthesis process is required in order to remove the templates; secondly, the nano-structured polymers may be destroyed or form

undesirable aggregated structures after released from the templates. Typically, the hard templates were firstly immersed in a precooled acidic solution of aniline, and the oxidant solution at the same temperature was added then to start the polymerization. During the procedure, PANI was produced and deposited within the pores or channels of the templates. With the templates eliminated, partly or completely, one-dimensional nano-structured PANI was isolated. Occasionally, the templates were not removed; giving rise to the one-dimensional nano-structured PANI filled composite materials. In some cases, aniline was adsorbed from vapor phase into the channels of the templates, and polymerization was then carried out in an identical fashion as mentioned above. PANI nanotubules were also synthesized by placing solutions of aniline and ammonium peroxydisulfate (APS), the oxidant, in a two-compartment cell with the particle track-etched membrane (PTM) as the dividing wall, which serves as the hard template. The monomer and the oxidant diffused toward each other through the membrane and reacted, yielding the PANI nanotubules in the pores of the membrane. In addition to the above-mentioned chemical oxidative polymerization, PANI nanofibers, nanotubules and nanoribbons were also prepared by electrochemical oxidative polymerization with hard templates such as PTM, AAO and enclosed nanochannels. With an alumina membrane as the hard-template, PANI nanotubules encapsulated nickel nanowires were prepared by Cao *et al.* (Cao, Tie, Xu, Hong, Sang 2001) through a two-step process. The nickel nanowires were protected from corrosion and oxidation in air by the PANI nanotubules, rendering the nano-structured composite promising material for some applications such as microelectronics and magnetic antenna material. Inorganic particles, such as Ni particles, were also used as templates in synthesizing PANI nanofibers.

2.3.1.1.2 Soft Template Synthesis

The soft template synthesis method, always called the template-free method or self-assembly method in the literatures in that no hard templates is used, entails synthesizing the PANI, as well as polypyrrole, in the presence of structure-directing molecules such as surfactants, deoxyribonucleic acid (DNA), polyelectrolytes, thiolated cyclodextrins, sulfonated porphyrin, liquid crystalline, and ethanol, which act as templates for production of the one-dimensional

nanomaterials. The surfactants are often complex acids with bulky side groups, such as the naphthalenesulfonic acid (NSA), camphorsulfonic acid (CSA), azobenzenesulfonic acid (ABSA), chiral 2-pyrrolidone-5-carboxylic acid (PCA), 4-(3-(4-((4-nitrophenyl)azo)phenyloxy)propyl)aminobenzene sulfonic acid (C3-ABSA), 2-acrylamido-2-methyl-1-propanesulfonic acid (AMPSA), 5-aminonaphthalene-2-sulfonic acid (ANSA), etc. The polyelectrolytes include poly(acrylic acid), poly(styrenesulphonic acid), etc.. The method is simple and cheap in comparison with the hard template method because it omits the use of the hard templates and therefore the wearisome post synthesis processing. The formation of the one-dimensional nano-structured PANI depended on the reaction conditions, such as the concentration of aniline, the molar ratio of aniline to oxidant or the soft template. Generally, the lower concentrations of aniline favored the formation of nanotubes or nanofibers, while the higher concentrations did the granular PANI. In a typical surfactants based procedure, aniline and surfactants such as CSA, NSA, ANSA, *o*-aminobenzenesulfonic acid etc. with different molar ratios were added to a certain amount of distilled water. A transparent solution of aniline/surfactant salt was formed and was brought to a specified temperature. Then an aqueous solution of oxidant, usually APS, pre-cooled to the same temperature was added to the above transparent solution to initiate the polymerization. After a predetermined period of reaction time, the mixture was filtered, washed, and dried to obtain the one-dimensional nano-structured PANI. For instance, Wan's group prepared both nano- and micro-structured PANI tubes (Long, Chen, Zheng, Wang, Zhang, Wan 2003), as well as polypyrrole tubes (Liu, Wan 2001), with various acids by this method. Yang *et al.* (Yang, Wan 2002) synthesized chiral PANI nanotubes with inner diameter of 50–130 nm, outer diameter of 80–220 nm and aspect ratio of 6–10, with chiral PCA as the template. Nickels et al.(Nickels, Dittmer, Beyer, Kotthaus, Simmel 2004) and Ma et al. (Ma, Zhang, Zhang, He 2004) synthesized nanowires of PANI with DNA as the template, and the nanowires were immobilized on silicon surface with pre-stretched strand DNA as the template. Very recently, Li et al. (Li, Pang, Peng, Wang, Cui, Zhang 2005) prepared PANI nanofibers with diameters of 100–120 nm and lengths of several micrometers with *p*-aminobenzenesulfonic acid as the surfactant, and the diameters of the nanofibers

decreased with decreasing of the *p*-aminobenzenesulfonic acid concentrations. Self-doped PANI nanofibers with a diameter of 120–370 nm were synthesized by Yang et al. (Yang, Chih, Cheng, Chen 2005) with *o*-aminobenzenesulfonic acid, a self-doping monomer, as the surfactant. In another surfactants based procedure, aniline was polymerized in acidic solution, including both the inorganic acids such as hydrochloride acid (HCl), H_2SO_4, HBF_4 and H_3PO_4, and organic acids such as AMPSA, in the presence or absence of the surfactants, such as sodium dodecylbenzene sulfonate (SDBS) and hexadecyltrimethylammonium bromide (HTAB), Triton X-100 or Allura Red AC to prepare one-dimensional nano-structured PANI. Both nanotubes/nanorods with average diameter of 150–340 nm and nanofibers with average diameter of 56 nm were obtained. Different dopant anions can be introduced to the nanomaterials by a dedoping–redoping procedure without significant changing of the morphologies and diameters of the nanostructures. Concerning the formation mechanisms of the nanostructures, it was proposed, but not confirmed, that the surfactants self-assembled with or without their aniline salts into nano- or micro-structured intermediates due to the hydrophobic property of aniline and the hydrophilic property of the surfactants, which played a template role in forming of the one-dimensional nano-structured PANI. The diameters and lengths of the one-dimensional nano-structured polymer were depended on the factors such as the soft templates, molar ratio of surfactant to aniline, reacting temperature and time and other synthetic conditions. For example, when the molar ratio of CSA to aniline was fixed at 2, granular PANI was formed, while in decreasing of the ratio from 1 to 0.01, tubular PANI was produced with diameters decreased from 180 to 85 nm. The same result was obtained with NSA and ANSA as the soft templates. With decreasing of the molar ratio of NSA to aniline from 2 to 1 and 0.5, tubular PANI with average diameters of 650, 154 and 92 nm, respectively, was obtained. While with further decreasing of the ratio to 0.25, nanofibers with average diameters of 76 nm were produced. In the case of ANSA, irregular granular PANI was obtained when the molar ratio of ANSA to aniline falls in the range of 0.25–0.5. While decreasing of the ratio to 0.1 and 0.02, very short PANI cylinders and PANI nanotubes with outer diameter of 60–100 nm were observed, respectively, and both coexisted with granular

PANI. Besides, adding of water to the aniline/surfactants systems before initiation of polymerization decreased also the diameters of PANI tubes from micrometers to nanometers. In spite of the above-mentioned proposals and results on the formation of PANI nanostructures, Konyushenko et al. (Konyushenko, Stejskal, Sedenkova, Trchova, Sapurina, Cieslar, Prohes 2006) pointed out recently that morphology of PANI depends on the acidity conditions during the reaction rather than on the chemical nature of the acid adopted. For example, granular PANI was produced when the polymerization was carried out in solutions of sulfuric acid, while PANI nanotubes with external diameter of 100–300 nm and internal diameter of 20–100 nm, and length of several micrometres were obtained in solutions of acetic acid. While in a polyelectrolyte based procedure, the polyelectrolyte was firstly dissolved in an organic solvent, such as tetrahydrofuran, to give a homogeneous solution. Aniline was then added to the solution to form a gel composed of a molecular complex of aniline and the polyelectrolyte. After washed with tetrahydrofuran to eliminate the excess of aniline, the gel complex was re-dissolved in an acidic aqueous solution. Following the addition of the oxidant solution, polymerization was initiated. Reacted for a specific period of time, PANI nanofibers were collected by filtration. As far as the mechanism is concerned, it was suggested that aniline was firstly bound onto the polyelectrolytes, followed by polymerization of aniline attached to the polyelectrolyte templates. Therefore, PANI nanofibers with diameters of 50 nm were produced when the template molecule is an extended linear chain of poly(acrylic acid), while globular morphology was obtained when the random coil conformation of poly(styrenesulphonic acid) was used as template. One-dimensional nano-structured PANI was also reported during electrochemical polymerization of aniline with thiolated cyclodextrins, sulfonated porphyrin, liquid crystalline, or ethanol, as the soft templates. Modified the gold electrodes with self-assembled monolayer of thiolated cyclodextrins, Choi and Park (Choi, Park 2000) prepared both nanowires of PANI with diameter of *ca.* 70 nm and length of 1.5 μm, and nano-rings of PANI with diameter of ca. 85 nm and length of 3.4 μm. The potentiodynamically grown nanowires exhibited much smoother morphology with fewer defects and longer lengths than those galvanostatically grown ones. When liquid crystalline was adopted

as the template, PANI nanowires with diameter of 50–70 nm and lengths of several microns were obtained. The distance between the working electrode and the counter electrode played an important role in depositing high quality nanowires. Generally, reduction of the distance favored better alignment of the liquid crystalline, and therefore well ordered and longer nano-wires of PANI. In the case of ethanol as the template, PANI nanofibers with diameters smaller than 100 nm were obtained and it was revealed that both the electric quantity in electropolymerization and the ethanol affected the morphology of the final PANI. For example, 90% (area fraction in SEM images) of nanofibers with diameters of 20–50 nm was observed on platinum deposited quartz substrate electrode with 30 min of polymerization, while fibers with diameters larger than 100 nm were obtained with polymerization time of 15 min. The reason for the formation of nanofibers was, on one hand, the ethanol molecules wrapped the PANI particles due to the strong H-bonding between them and prevented thus the aggregation of PANI particles during their polymerization, on the other hand, the increased forming rate of crystalline nucleus due to the presence of ethanol is □ on-volati for electrosynthesizing of PANI nanofibers. Thanks to the one-dimensional aggregation structures of 5,10,15,20-tetrakis(4-sulfonatophenyl)-porphyrin in water, nanorods of PANI with diameters of 20–50 nm and lengths of 200–1000 nm were also prepared by electrochemical oxidative polymerization in the presence of sulfonated porphyrin with various porphyrin concentrations. The aspect ratios of the PANI nanorods were affected by the sweeping potentials and cycles. The "density" of the PANI nanorods, i.e. the crowdedness of the nanorods, increased with the concentrations of porphyrin, indicating that the aggregated sulfonated porphyrin functioned as soft template in directing the morphology of PANI. Additionally, the equilibrium adsorbed surfactant aggregates can also be used as soft templates for synthesizing nanostructured PANI, as well as polypyrrole, with controlled morphology on flat surfaces. Aniline and sodium dodecyl sulfate (SDS), a kind of surfactant, were allowed to aggregate on highly oriented pyrolytic graphite surfaces in the first step, and then the oxidant was added to start the polymerization. Finally, the substrate was rinsed to remove the excessive ingredients, resulting well aligned PANI nanowires parallel to the surface, as well as other morphologies on the substrates.

More importantly, uniform dendritic PANI nanofibers, with diameters and lengths of 60–90 nm and several hundreds of nanometers, respectively, were chemically synthesized with a special surfactant gel formed by a mixture of hexadecyltrimethylammonium chloride (C_{16}TMA), acetic acid, aniline, and water at −7°C. The lengths of the PANI branches decreased with decreasing of the C_{16}TMA concentration, and finally PANI nanoparticles were resulted with a C_{16}TMA concentration of 0.05 mol/L. However, when the C_{16}TMA was replaced by cetyltrimethylammonium bromide (CTAB), PANI nanobelts with thickness, width, and length in the range of 40–50, 300–400 nm, and about several micrometers, respectively, were prepared by the same group at −7°C with the concentration of CTAB vary from 0.05 to 0.25M. Note that only PANI nanoparticles with diameters of 70–100 nm were obtained with 0.25M CTAB when the synthesis was carried out at room temperature, it was assumed that the surfactant played a template-like role in the synthesis of PANI nanobelts.

2.3.1.1.3 Combined Soft and Hard Template Synthesis

In order to fabricate highly oriented PANI nanostructures, a novel method combing the soft and hard template synthesizing technique was employed. Typically, aniline and the surfactant, e.g. C3-ABSA, was dissolved in deionized water to form a homogenous emulsion and ultrasonicated for a while. The hard template, e.g. a porous, hydrophilic Al_2O_3, was immersed in the emulsion and ultrasonicated for another while. Afterwards, the APS solution was added rapidly to initiate the polymerization. With different reacting time, the oriented PANI nanotubes and nanofibers were produced within the pores of the hard template. No oriented nanofibers was obtained neither with NSA as the soft template nor with a hydrophobic Al_2O_3 as the hard template solely, revealing that both the dopants and the surface property of the hard template affect the alignment of PANI nanofibers or nanotubes. The fact that one nanotube or nanofiber was grown in a regular hexagon shaped pore, and two or more in a irregular shaped pore, differing from the fact that one fiber or tube in one pore during the direct use of Al_2O_3 as the hard template, indicated that both the soft and hard template affected the formation of the nanofibers

or nanotubes. The lengths of the nanofibers or nanotubes can be roughly controlled by varying the polymerization time.

2.3.1.1.4 Seeding Polymerization

By adding a small amount of various nanofibers like the PANI nanofibers in diameter of ~50 nm, the single-walled carbon nanotubes bundles in diameter of ~ 20 nm, nanofibrous hexapeptide in diameter of ~12 nm, and the V_2O_5 nanofibers in diameter of ~15 nm, into the reacting solution of aniline and APS, Zhang et al. (Zhang, Goux, Manohar 2004). Invented the so-called "nanofiber seeding" method for preparation of PANI nanofibers. Typically, about 1–4 mg of these seeding nanofibers were added firstly into a stirred solution of aniline (0.14 M) in hydrochloric acid (1.0 M), and a solution of 0.04M APS was added then to the mixture to initiate the polymerization. The resulting dark-green precipitate of PANI was isolated after 1.5 h and dried under dynamic vacuum. The morphology of all the seeded PANI products was fibrillar with fiber diameters in the range of 20–60 nm. In contrast, when the reaction is seeded with spheres, for example, the particulate PANI and the nanospheres of polypyrrole, nanofibrous morphology was obtained just like that in the unseeded reaction. One of the advantages of the seeded approach is that bulk quantities of doped PANI nanofibers could be produced in one step without the need of conventional templates, and hence the need for tedious post-processing. Besides, PANI oligomers, Au nanoparticles with average diameters of 15 nm and carbon nanotubes were also used as the "seeds" in preparing PANI nanofibers. Very recently, Zhang et al. (Zhang, Kolla Wang, Raja, Manohar 2006) confirmed that the PANI nanofibers prepared in chemical oxidative polymerization with APS as the oxidant were resulted from the rodlike structure of anilinium–peroxydisulfate ion clusters formed during the induction period, which acted as the in situ generated seeds in directing the morphology of the final product.

2.3.1.2 No-template Synthesis

To distinguish from the commonly called template-free synthesis of the soft template synthesis method, the phrase "no template synthesis" was coined here to name the method for synthesizing one-dimensional nano-structured PANI without any templates, hard or soft.

2.3.1.2.1 Interfacial Polymerization

Initially, PANI or its composite films were produced via interfacial polymerization approach in which aniline was codissolved with the surfactant or polymers in the organic phase, while APS in aqueous acidic phase, giving rise to the films at the interface of the two immiscible liquids. However, both nanofibers and nano-particles of the polymer were produced recently, rendering the approach one of the general and facile among a variety to synthesize one-dimensional nano-structured PANI. In a typical reaction, aniline was dissolved in the organic phase, which can either be one with density lower than water such as hexane, benzene, toluene, etc. or be one higher, such as carbon tetrachloride, methylene chloride, etc., with various concentrations. Meanwhile, APS was dissolved in an aqueous acid solution, covering a great variety of acids such as HCl, sulfuric acid, CSA, toluene sulfonic acid, among others. And then, the two solutions were gently transferred to a reaction vessel such as a beaker or a vial, generating an interface between the two layers. Green PANI was formed firstly at the interface as the reaction proceeds and migrated gradually into the aqueous phase until the whole aqueous phase is filled homogeneously with dark-green PANI at last. Finally, the aqueous phase was collected after sufficient time of reaction by dialysis or filtration to remove the impurities like excess dopants, etc., yielding PANI nanofibers in the form of a water dispersion or powder. Dedoped PANI nanofibers can be obtained by further washing or dialyzing with ammonia. In consideration of the formation mechanisms, it was revealed that interfacial polymerization suppressed effectively the secondary growth of PANI, which occurred naturally in the conventional synthesis of PANI, leading thus to the exclusive formation of nanofibers. The monomer and oxidant, separated in two phases, met only at the interface and reacted there then, forming PANI nanofibers. The nanofibers formed moved away rapidly from the interface and diffused into the water phase due to their hydrophilicity. As such, the nanofibers were continuously withdrawn from the interface, allowing formation of new nanofibers at the interface. As far as the synthesizing parameters (such as the solvents, polymerization temperature, and monomer concentration) are concerned, it was demonstrated that all aqueous/organic systems produce similar PANI nanofibers, whose morphology was

unaffected in the subsequent dedoping process. However, both the diameters and the quality/uniformity of the nanofibers were affected by the acids and their concentrations. For example, the average diameters of the fibers synthesized in HCl, CSA, perchloric acid, and other acids (such as sulphuric acid, nitric acid and 4-toluenesulfonic acid) are 30, 50, 120, and 30–50 nm, respectively. In the case of strong acids like HCl and CSA, the lower the concentration of the acid, the lower the fraction of nanofibers in the final product. While in the case of medium or weak acids like tartaric acid or pyrrolidone-5-carboxylic acid, the products were mixtures of nanofibers and particles even at high concentrations. It was therefore stated that high concentrations of strong acids favored the formation of PANI nanofibers. The diameters of the nanofibers prepared by interfacial polymerization can be controlled by using surface active dopants like AMPSA or CSA, and surfactants in the aqueous phase. The surfactants cover the single-tailed non-ionic ones like octylphenol ethoxylate Triton-X 100 and d-Alpha Tocopheryl Polyethylene Glycol 1000 Succinate (Vitamin E TPGS), the single-tailed anionic ones like DBSA, and the twin-tailed ones like potassium *cis*-1,2-dipentylethene sulfonate (C_5H_{11}-twintailed), potassium *cis*-1,2-diheptylethene sulfonate (C_7H_{13}-twin-tailed) and sodium di(2-ethylhexyl) sulfosuccinate aerosol-OT (AOT). Solutions of the surfactants, if used, were gently syringed into the aqueous phase layer, i.e. bottom phase in the case, just below the interface. The average diameter of the fibers obtained using 1.0 M AMPSA as the aqueous phase is ~ 23 nm, smaller than the ~ 48 nm for the fibers obtained with 1.0M CSA as the aqueous phase. The reason was expected to originate from the more efficient packing capability of AMPSA than that of CSA due to its more linear structure. In the case of the CSA based nanofibers, the single-tailed non-ionic surfactants increased the average diameter to ~ 80 nm, while the single-tailed anionic surfactants seemed to have no any impact on fiber diameter. However, the twin-tailed surfactants increased the average diameter to ~ 30 nm, and the longer the alkyl chain length, the smaller the average diameters. For instance, the average diameters of the CSA based nanofibers synthesized with no surfactant, with C_5H_{11}-twin-tailed and C_7H_{13}-twin-tailed as surfactants are 48, 35 and 28 nm, respectively. While in the case of the AMPSA based nanofibers, this trend of the alkyl chain effect was reversed. The

average diameters increased from 23 nm (no surfactant) to 35 nm and 55 nm with C_5H_{11}-twin-taile and C_7H_{13}-twin-tailed as the surfactants, respectively. Although these surfactants might be expected to disrupt the intrinsic packing properties of the AMPSA, the reason for this reversed alkyl chain effect is not clear up to now. And aside from the above-mentioned morphological effect, the average doping percentage of the PANI nanofibers was lowered with addition of the twin-tailed surfactants during interfacial polymerization. By placing an Au substrate with self-assembled monolayer of 4-aminothiolphenol at the interface of an interfacial polymerization, Hopkins and coworkers (Sawall, Villahermosa, Lipeles, Hopkins 2004) grafted a two-dimensional mesh of PANI nanofibers with diameters of 40–50 nm onto the Au surface through the covalent bonding between PANI and the amine created by the 4-aminothiolphenol monolayer. It was of a great attempt to pattern the one-dimensional nano-structured PANI onto substrates in an ordered form. In contrast to other nano-patterning techniques of PANI on Au surfaces, the method exhibited both improved physical (adhesion) and chemical (little changes of conductivity to a series of acid/base exposure) durability. With sulfonated polystyrene as both the host and the dopant in interfacial polymerization, the same group prepared transparent conductive nanocomposites with well-defined two-dimensional PANI nanofibers, rendering the procedure a unique and facile one in preparing robust conductive PANI nanofibers-based composites.

2.3.1.2.2 Radiolytic Synthesis

In this method, the aqueous solution of aniline and APS in HCl was irradiated with gamma rays without any template. In the case of parent solutions with typical concentration of 0.1M aniline, 0.3M HCl, and 0.002–0.1M APS, the morphology of the final product was predominantly nanofibers with diameters of 50–100 nm and length of 1–3 μm, though less than 5–vol.% of globular structures were still presented. While with APS concentrations in the range of 0.05–0.1M in the parent solution, rodlike structures with diameters of 250–500 nm and lengths of 5–10 μm were observed, which represent 5 vol.% of the total PANI. The selected-area electron-diffraction of the rodlike structures was comparable to that of the nanofibers, which are poorly ordered. Fourier transform infrared (FTIR) spectrum

agreed well with that of the typically prepared PANI, indicating that the chemical structure of the fibers was not affected by irradiation. No complete explanation for formation mechanism of the nanofibers was provided up to then according to the authors. However, the authors concluded that PANI self assembled when the polymerizationwas carried out with gamma irradiation. In addition, four to five times larger sized spherical aggregates, as compared with the aggregate diameters of 20–40 nm without irradiation, and hollow spheres with diameters of 50–100 nm were observed with irradiation. The hollow aggregates tended to stick to and link spheres, which coalesced then in an anisotropic fashion and resulted then, probably, the nanofibers. PANI nanofibers decorated with metal nanoparticles were also prepared with the same gamma irradiation procedure. At the same time, thin films of PANI nanofibers were synthesized by the same group by ultraviolet irradiation of a spin coated mixture of aniline nitric acid and APS on the surface of a siliconwafer. The nanofibers demonstrate typical diameters of 20–150 nm and lengths of microns.

2.3.1.2.3 Rapid Mixing Reaction

With the solution of APS mixed rapidly with that of aniline, rather than the conventional slow addition of the solution of APS to that of aniline, PANI nanofibers with comparable shapes and sizes to those of interfacial polymerization method were obtained, rendering this method the simplest one in producing PANI nanofibers. Owing to the even distribution of aniline and APS molecules in the solution, all the initiator molecules were consumed rapidly after the start of the polymerization and the secondary growth of PANI was suppressed, resulting exclusive nanofibers in the product. The growth of the PANI nanofibers was related with the polarity of the solvents. For example, in aqueous systems, pure nano-fibers were produced, while in ethanol and isopropanol, mixture of short nanofibers attached with irregular particles and agglomerates of 100–300 nm particulates were obtained, respectively. However, according to Zhang et al. (Zhang, Wei, Wan 2002), the formation of nano-structured PANI, which was synthesized in presence ofH_3PO_4 without any other template, soft or hard, was expected to originate from the micelles formed by anilinium cations, which acted as the tem plates in forming the nanostructures. In another similar study, chloroaurate acidwas used as the oxidant.

PANI nanofibers with diameters of 35±5 nm and gold nanoparticles in diameters of 30–40 nm were obtained. The formation of the nanofibers was probably owing to the catalytic effect of the gold nanoparticles in directional growth of the PANI, though the exact growth process of the nanofibers was not clear. Chiou and Epstein (Chiou, Epstein 2005; 2005) prepared PANI nanofibers by dilute polymerization, in which a small portion of acid solution containing aniline was carefully transferred to the solution of APS in acid and then leave the mixture to react without any disturbance. The diameters of the fibers can be roughly tuned by appropriate selection of the acids. For instance, when CSA, methanesulfonic acid and perchloric acid were used, the diameters of the fibers were in the range of 17–50, 42–70 and 72–250 nm, respectively. The formation of the nanofibers was as explained, owing to the reduced numbers of nucleation sites on the surface of the nanofibers in a dilute condition, which allowed PANI to grow directionally, differing from that of the competition between the directional growth and the formation of additional nucleation centers in the case of high aniline concentration, which resulted irregular PANI product. Very recently, Li and Kaner (Li, Kaner 2006) pointed out that the formation of PANI nanofibers was a result of homogeneous nucleation during the synthesizing process, differing from the above mentioned proposals. At the initial stages, PANI nanofibers with smooth surfaces and uniform sizes were formed in the reaction system via a homogeneous nucleation. When the system was mechanical stirred, the primarily formed PANI nanofibers were forced to collide into each other and heterogeneous nucleation occurs on the surfaces of these particles, causing aggregations of the primary nanofibers; while when the system was left still, the heterogeneous nucleation was suppressed and nanofibers were produced continuously. The proposed mechanism appears to hold for other materials such as poly(*m*-toluidine) and silica nanoparticles as per the authors. Besides, in absence of stirring, the higher temperature favors more the homogeneous nucleation owing to the faster formed embryonic nuclei than the lower temperature. For instance, PANI nanofibers formed at 60 °C is more uniform than that formed at 0 °C.

2.3.1.2.4 Sonochemical Synthesis

By dropwise addition of an acidic APS solution to an acidic aniline solution, just like the conventional PANI synthesis procedure, with the aid of ultrasonic irradiation, PANI nanofibers with higher polymer yields were successfully prepared by Jing et al. (Jing, Wang, Wu, She, Guo 2006). It was stated that three possible competitions exist in the reaction system if more aniline and APS are present following the formation of the primary PANI nanofibers, i.e. (1) the continuing formation of primary PANI nanofibers, (2) the growth of the primary nanofibers into unevenly surfaced thicker fibers, and (3) the growth and agglomeration of the thicker fibers into irregular particles. In the conventional procedure, irregular PANI particles were obtained owing to the continually occurring of steps (2) and (3); while in the case of sonochemical synthesis, the further growth and agglomeration of the primary nanofibers were effectively prevented, even more aniline and APS were added into the system, resulting to the formation of more primary PANI nanofibers. One of the advantages of the approach is its scalability in comparison with others such as interfacial polymerization or rapid mixing reaction.

2.3.1.2.5 Electrochemical Approach

Aside from the above-mentioned chemical no-template approaches, one-dimensional nano-structured PANI was also synthesized by electrochemical no-template approaches. PANI nanofibrils, as well as microfibrils or rods, have been found by Langer et al. (Langer, Czajkowski 1997) in electrochemically synthesizing PANI from an aqueous medium at pH ~1 without any templates. The nanofibrils doped with fullerene derivatives exhibited diameters of 10–100 nm and lengths of 500–2000 nm. Both single nanofibrils and their networks were obtained with controlled charge flows. Latterly, large arrays of uniform and oriented nanowires of PANI with diameters less than 100 nm were synthesized by Liang et al. (Liang, Liu, Windisch, Exarhos, Lin 2002) on a variety of substrates by a three-step electrochemical deposition procedure, also without using any templates. Typically, a large current density was adopted for a while (0.08 mA/cm^2 for 0.5 h) to create the nucleation sites on the substrates in the first step; in the second step, a reduced current density was followed (0.04 mA/cm^2 for 3 h); finally, a much reduced current

was followed (0.02 mA/cm^2 for 3 h). The stepwise growth produced uniform and oriented nanowires on both flat substrates and particles and textured surfaces. For example, nanowires with diameters of 50–70 nm and lengths of 800 nm were formed perpendicular to a Pt substrate. When the substrates were colloidal silica particles, the nanowires produced were oriented perpendicular to the particle surfaces. PANI nanowires were also fabricated to bridge a sharp scanning tunneling microscope tip and an Au electrode by electrochemical polymerization, and the diameter can be reduced by mechanical stretching of the nanowires. For example, assuming the volume of the nanowires does not change during stretching, the upper limit diameter of the PANI nanowires can be reduced from the initial ~ 20 to ~ 6 nm by stretching over a distance of 200 nm. With porous poly(styrene-block-2-vinylpyridine) diblock copolymer films as the templates, which were spin coated to the electrode and then treated with acetic acid before hand, highly porous PANI nanofiber films were also prepared by electrochemical approach.

2.3.2 Properties of Polyaniline Nanostructures

As revealed by the FTIR spectra, UV–vis spectra, and the X-ray diffraction, all the PANI nanotubes, nanofibers, nanowires, nanorods, as well as microtubes, have backbone structures similar to that of the conventional prepared granular PANI. In some cases, the Einstein shifts observed in the FTIR and UV–vis spectra were originated from the interaction between the PANI chains and some small molecules, such as ethanol, not from the chemical structures. For electrochemical prepared oriented PANI nanowires, polarized infrared spectroscopy suggested that the PANI molecules were aligned perpendicular to the axis of the nanofibers. For the hard-template synthesized PANI nano- and microtubes/fibers, they exhibited a highly ordered layer (ca. 5 nm in thickness) on the outer surface, in which the PANI chains are aligned perpendicular to the axis of the nano- or microstructures, and progressively disordered layers toward the center of the nano- or microstructures. Conductivity measurement of the hard-template synthesized PANI nanotubules showed that the conductivities decreased with the increasing of the diameters, and finally reaches the conductivity of the conventional PANI powder. This was resulted

from the decreasing proportion of the highly ordered layer in the materials with increasing of diameters and from the higher conductivity of the highly ordered layer than that of the disordered inner part of the fibers/tubes. The analogous conductivity decrease was also observed for electrochemically template-synthesized PANI nanoribbons. The four-probe conductivity of the PANI pellet consisting of both granular particles and nanofibers, or the PANI nanofibers pellet was similar to their counterpart synthesized by the conventional procedure, and was affected by the doping acid and doping degree, and so on. The directly measured electrical conductivity of a single PANI nanotube, which was synthesized by the soft template method, is ca.30 S/cm, far more higher than the 10^{-2} S/cm order of magnitude for the nanotube pellet due to the large intertubular contact resistance. Brunauer–Emmett–Teller (BET) surface area of the PANI nanofibers decreased with increasing of the fiber diameters. For example, BET surface area of dedoped PANI nanofibers with diameters of 30, 50, and 120 nm are 54.6, 49.3, and 37.2 m^2/g, respectively. In addition, the BET surface area of doped PANI nanofibers was lower than that of the dedoped ones, which is in consistent with the results of the conventional PANI.

2.3.3 Application of Polyaniline Nanostructures

Apart from the above-mentioned similar properties of the one-dimensional nano-structured PANI to that of the conventional granular PANI powders, several unique properties, such as large surface area, were exhibited by the one-dimensional nanostructured PANI, rendering this important class of new materials promising candidates for applications ranging from sensors to energy storages and electron field emissions.

2.3.3.1 Sensor Application

The electrical conductivity changing of PANI, as well as other intrinsically conducting polymers, upon exposure to acidic or basic vapors and liquids, such as HCl, ammonia gas, or ammonia water, CO_2, as well as some neutral gases including chloroform, alcohols, etc., rendered PANI one of the novel promising materials for sensor applications, and tremendous works have been undertaken on the field. However, poor sensitivity resulted from the poor diffusion of analyte molecules

was observed for the conventional PANI and the composite films. One dimensional nano-structured PANI enhanced significantly the diffusion due to its greater exposure area and penetration depth for gas molecules than the conventional PANI, and became an alternative material to improve the sensitivity of PANI based sensors, especially for acidic and basic gases. For example, the resistance response of the interfacial polymerized PANI nanofibers based film was much faster than that of the conventional PANI based film on exposure to 100 ppm of HCl and NH_3, although the nanofibers based film is more than twice in thick. In addition, the response and corresponding sensitivity of the nanofibers based film was independent on the thickness owing to its porous nature which facilitate the interaction of molecules with all the fibers, outside and inside of the film. On the other hand, the performance of the conventional PANI film was strongly thickness dependent. The thinner the film, the better the performance in that only the outmost surface interacts with the □ on-vo molecules. In the case of neutral gas molecules, such as hydrazine, methanol and water, PANI nanofibers based films exhibited faster responses, but lower sensitivity than the conventional PANI film. The reason lied in both the relatively "open" structure of the polymeric materials as compared with metal or inorganic materials and the adverse effect from the interfibrillar contact resistance of the nanofibers based films. If chirality, which originate only from the helical conformation of polymer backbone and/or from the helical packing of the polymer chains induced by chiral acids due to the absence of asymmetric carbon in doped PANI, was imparted to the PANI nanofibers with high surface areas, chiral separation and biological sensors would be the new potential areas for applications of the nanofibers. The well-aligned PANI nanowires were also tested as support materials for sensing applications due to their oriented microstructure and high surface area. Iron hexacyanoferrate, an active ingredient for H_2O_2 detection, was electrochemically deposited in form of nanoparticles on oriented PANI nanowires to fabricate H_2O_2 sensors. The presence of the PANI improved the stability of the iron hexacyanoferrate and lowered the over-potential of H_2O_2, which are of great importance in practical sensing and detecting of H_2O_2. The stable, reliable and almost linear response of the composite sensor proved

the iron hexacyanoferrate loaded PANI nanowires a useful configuration for H_2O_2 sensors.

2.3.3.2 Energy Storage

PANI nanofibers showed higher capacitance values and more symmetrical charge/discharge cycles due to their increased available surface area, in spite of their similar redox peaks displayed in aqueous electrochemistry to that of the conventional granular PANI. For example, a capacitance value of 122 F/g was achieved for HCl doped PANI nanofibers, far higher than the 33 F/g in the conventional prepared HCl doped PANI powder. These kinds of specific properties of PANI nanofibers could be beneficial to development of the next-generation energy storage devices.

2.3.3.3 Field Emission Application

Well-aligned PANI nanofibers, in shape of membrane together with the hard template of AAO, were directly tested as electron field emitter. The stable field emission, low threshold voltage (5–6 V/μm) and high emission current density (5 mA/cm^2) of the membrane suggested the material an attractive field-emitting candidate. Furthermore, the easy preparation, smooth and substantial surface, low cost, and good mechanical property of the material will be favored in fabrication of field emission displays.

2.3.3.4 Flash Welding

Irradiated by a camera flash, a random network of PANInanofibers was turned into a smooth and shiny film due to the highly efficient photothermal conversion and low thermal conductivity of PANI, which demonstrated a versatile new technique for processing polymers into potentially useful structures. One of the great advantages of the flash welding technique is that a certain area can be selectively welded by using of a photomask in fabricating polymer films into pre-designed patterns, differing from other welding techniques like microwave welding. In addition, the technique offered a rapid route in creating asymmetric films, which are widely used in many applications such as separation membranes, chemical sensors and actuators.

2.3.3.5 Digital non-volatile Memory

PANI nanofibers (~ 30 nm in diameters) decorated with Au nanoparticles (~ 1 nm in diameter) were also attempted for fabrication of plastic digital memory device. The device exhibited very interesting bistable electrical behavior and can be switched electrically between two states with a conductivity difference of about three orders of magnitude. The switching mechanism was attributed to an electric field-induced charge transfer from the PANI nanofibers to the Au nanoparticles. The prolonged retention time and good write-read-erase cycle results suggested the device promising for digital non-volatile memory.

2.3.4 Literature Review of Polyaniline Nanoparticles

Mazur *et al.* (2003) synthesized the polyaniline and poly(2-methoxyaniline) nanotubes by chemical *in-situ* deposition within the pore of polycarbonate membranes. The result showed that the polyaniline was first formed in the polymerization solution and then it precipitated on/into the membrane. In contrast, the oxidized poly(2-methoxyaniline) molecules were first absorbed on the polycarbonate surface, and then, as a consequence of their accumulation, they recombined to form the polymer.

Xiong *et al.* (2004) prepared the highly ordered polyaniline nanotubes by *in-situ* polymerization using the anodic aluminium oxide (AAO) as a template. The result suggested that the obtained polyaniline nanotubes array is the duplicatde of the channels of the AAO template. The forming mechanism was due to the electrostatic interaction of aniline molecular and pore walls of the template, which led to absorbtion, nucleation, and polymerization of aniline, preferentially on the pore walls of template.

Lu *et al.* (2005) presented the facial method to prepare the helical polyaniline microwires or rods guided by poly(acrylic acid). The helical wire- or rod-like products with the average length and diameter about 3.5 μm and 500 nm, respectively, and with the pitch distance about 400 nm were observed as the concentration of poly(acrylic acid) decreased to below 0.05 mg/ml.

Sarno *et al.* (2005) prepared the polyaniline nanofibers doped with 2-acrylamido-2-methyl-1-propanesulfonic acid by oxidative polymerization of aniline in the presence of a nonionic surfactant. It was found that the obtained nanofiber was possible to introduce the difference dopant anion from that used in the initial synthesis without significant changes in the fiber morphology or diameter via dedoping and redoping process.

Zhang *et al.* (2005) synthesized the polyaniline nanotubes doped with different naphthalene sulfonic acids (NSA) via self-assembly process. It was found that the formation yield, morphology, size, crystalline, and electrical conductivity of the nanostructures were affected by the position and the number of $-SO_3H$ groups attached to the naphthalene ring of NSA as well as the synthesis condition. Moreover these nanotubes aggregate to form a dendritic morphology when the polymerization was performed in the static condition. These aggregations were possibly due to the polymer chain interaction including π-π interaction, hydrogen and ionic bonding.

He (2005) synthesized the polyaniline microspheres with nano-meter sized aciculae by a solid state emulsion. It was found that the addition of $Cu_2(OH)_2CO_3$ nanoparticles could serve as the emusifiers to form and stabilize the emulsion in the water/toluene system. The spherical droplet of emulsion acted as the template for the formation of polyaniline microspheres whereas the polyanilne at the interfaces tend to elongate to wirelike shape after the APS was added.

Zhang *et al.* (2006) summarized the various synthesizing approaches of one-dimension nano-structure of polyaniline including the template synthesis and non template synthesis approaches. Moerover, they also reviewed several potential applications of the nanomaterials.

Xing *et al.* (2006) prepared the polyaniline nanofibers by using the conventional polyaniline in DMSO as a seed. They reported that the morphology and electrical conductivity of the obtained polyanilne nanofibers were dependent on the preparation conditions such as acid concentration, reaction time, aniline concentration, PANI/DMSO amount, PANI/DMSO concentration, and acid and oragnic solvent kinds. Moreover, they deduced that the seed played an important role to help forming, stabilizing and dispersing the polyaniline naofibers.

Wang *et al.* (2006) synthesized the polyanilne microfibers by using the $H_4SiW_{12}O_{40}$/polyacrylamide microfibers seeding template method. It was reported that the microfiber seeding template significantly affected the microfibrous morphology of the resulting polyaniline; however, the diameter of the polyanililine microfibers was not affected by the diameter change of the microfiber seeding template in their experimerntal range. The authors deduced that the poylmerization of aniline occurred only on the surface and overspread along the microfiber seeding template.

Sun *et al.* (2006) synthesized the dendritic superstructure of polyaniline by using a water-soluble polyelectrolyte copolymer as the dopant and support matrix. The formation of dendritic superstructure was attributed to the complexation between the polyelectrolyte and aniline oligomer functioned as nuclei and the nuclei directed the further growth of polyaniline to dendritic superstructure.

Li *et al.* (2006) synthesized the radially aligned polyaniline dendrites with the nanotubes junction using the tartaric acid as a dopant. These dendritic nanotubes with 80-400 nm in outer diameter, 30-50 nm in walls thichness, and several micormeters in length could form self-assemble into urchin-like nanostructures. The geometrical shape of the individual branch was a cone and the nanotubes junctions might provide the potential applications in nanoelectronic devices.

Chen *et al.* (2007) presented the novel interfacial polymerization method to prepare the radially oriented polyaniline nanofibers by using the salicylic acid as a dopant. The dimeter of the obtained polyaniline nanofibers were in range of 300-500 nm and these radially oriented polyaniline nanofibers might have the potential for microsensors or microelectronic and obtical devices.

2.4 Introduction to Polymer Rheology

The viscous flow of a Newtonian fluid is described by Newton's law of viscosity given for shear flow as

$$\tau = \mu \frac{d\gamma}{dt} \tag{2.1}$$

where τ is shear stress, μ is the Newtonian viscosity coefficient, and γ is the shear strain. The time dependence of shear strain is called the shear strain rate or shear rate:

$$\dot{\gamma} \equiv \frac{d\gamma}{dt}$$

A simple flow is defined as one in which only one of the three components of velocity a vector is nonzero.

$$\mathbf{u} = (u_1, u_2, u_3)$$

The subscripts 1, 2, and 3 identifying the three components of the velocity vector, u_i refer to the axes of the particular coordinate system used to analyze the flow process (i.e., x, y, and z in rectangular coordinates; r, θ, and z in cylindrical coordinates; and r, θ, and ϕ in spherical coordinates).

An example of a simple shear flow is Couette shear flow between two infinitely wide parallel plates, as illustrated in Figure 2.2. To analyze this simple flow, it is convenient to establish a rectangular-coordinate system having it x-axis fixed in bottom plate and oriented along the shear direction, with the y-axis perpendicular to the plate surface. In this case, the shear strain, γ, is defined as the ratio of deformation of a different element in the x-direction (dx) to that in the y-direction (dy) during shear, it is easily shown that the shear rate in plane Couette flow is equal to the velocity gradient as

$$\dot{\gamma} \equiv \frac{d\gamma}{dt} = \frac{d}{dt}\left(\frac{dx}{dy}\right) = \frac{d}{dy}\left(\frac{dx}{dt}\right) = \left(\frac{du_x}{dy}\right) \qquad (2.2)$$

where u_x is the velocity of the fluid in the x-direction. The maximum shear rate occurs at the moving plate surface and is given as U/H, where U is the constant (maximum) velocity of the upper plate moving in the x-direction and H is the distance of the separation between the two plates. The minimum shear rate is zero which occurs at the bottom (stationary) plate (i.e. $y = 0$) assuming there is no slip of the fluid layer at the plate surface; therefore, u_x (0) = 0. As illustrated in Figure 2.2, the velocity, u_x, is a linear function of the y-coordinate.

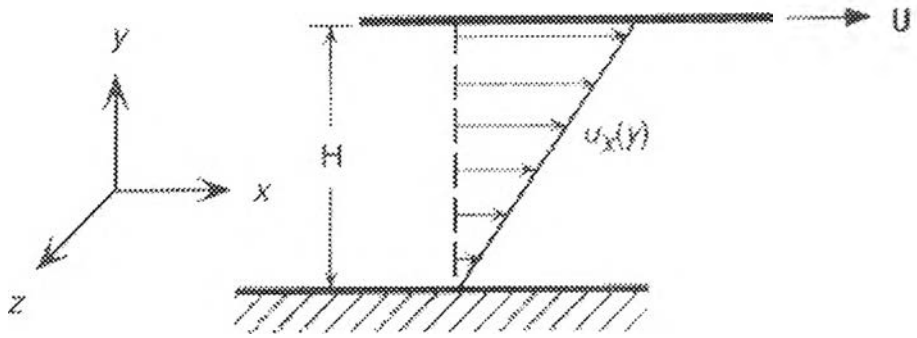

Figure 2.2 Representative of simple shear flow (plane Couette flow) between parallel plates whereby the upper plate is moving at a constant velocity (U).

In these case of Newtonian fluids such as water and mineral oil, the viscosity, μ, is a function of temperature an pressure but is independent of $\dot{\gamma}$ (shear rate). In contrast, the viscosity of non-Newtonian fluids such as concentrated polymer solution and polymer melts is a function of temperature, pressure, and $\dot{\gamma}$ (shear rate). In addition, the viscosity of polymer solutions and melts exhibits a strong dependence on molecular weight. These unique aspects of polymer rheology are discussed in the following section.

2.4.1 Non-Newtonian Flow

2.4.1.1 Shear Rate Dependence

A non-Newtonian or apparent viscosity.[†] η, of polymer solutions and melts is define following Newton's law of viscosity (eq. 2.1) as

$$\tau = \eta(\dot{\gamma})\dot{\gamma} \qquad (2.3)$$

Equation 2.3 is called the generalized Newtonian fluids (GNF) model. The actual analytical relationship between τ and $\dot{\gamma}$ and, therefore, the dependence of η and $\dot{\gamma}$ are given by the constitutive equation of the material. Melts of high-molecular weight polymers and their concentrated solutions display three characteristic regions as illustrated in Figure 2.3. At low shear rates, η is nearly independence of $\dot{\gamma}$ (i.e. Newtonian behavior) and approaches a limiting zero shear rate value of η_o. At higher $\dot{\gamma}$, η decrease with increasing $\dot{\gamma}$. Fluids that display this

behavior are termed shear-thinning. Finally, η once again approaches a limiting Newtonian plateau, at η_∞ very high $\dot{\gamma}$.

The molecular basis for shear-thinning behavior is the effect of shear on entanglements, as illustrated in Figure 2.4. At low shear rate, the entanglements impede shear flow and, therefore, viscosity is high. As shear rate increases, chain begin to orient in the flow direction and disentangle from one another — the viscosity begin to drop. Finally, the molecules become fully oriented in the flow direction at very high shear rates. At this point, stable entanglements are no longer possible and the viscosity reaches a lower level that is again independent of shear strain rate. This second Newtonian plateau region is observed in the case of polymer solutions but it is rarely observed for polymer melts, because shear rate required for chain orientation in the melt are so high that the chains actually can be broken (i.e. shear-induced degradation or mechanodegradation).

† Since τ and $\dot{\gamma}$ are shear stress and shear rate, respectively, the viscosity defined by eq. 2.3.

$$\eta \equiv \frac{\tau}{\dot{\gamma}}$$

is the shear viscosity. An extensional or Trouton viscosity is defined by the corresponding expression for tensile stress and strain as

$$\eta_T = \frac{\sigma}{\dot{\varepsilon}}.$$

The extensional viscosity and its dependence upon the tensile strain rate are important in modeling processing operations where significant extensional flow occurs, such as converging flow in a runner during injection molding and during calendaring and blow molding operations. Extensional viscosity may also have significant importance to the drag-reduction properties of dilute polymer solutions.

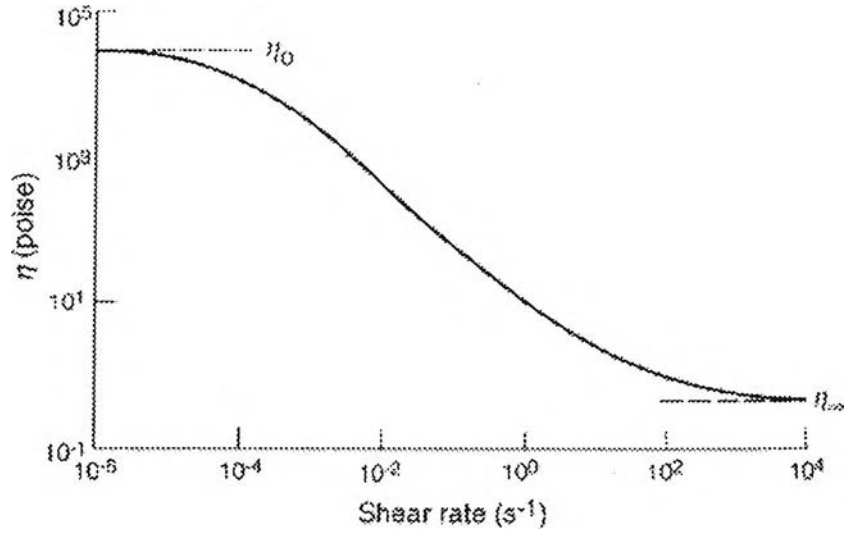

Figure 2.3 Typical dependence of apparent viscosity, η, of the polymeric melt on shear rate, $\dot{\gamma}$, showing the zero-shear viscosity, η_o, plateau.

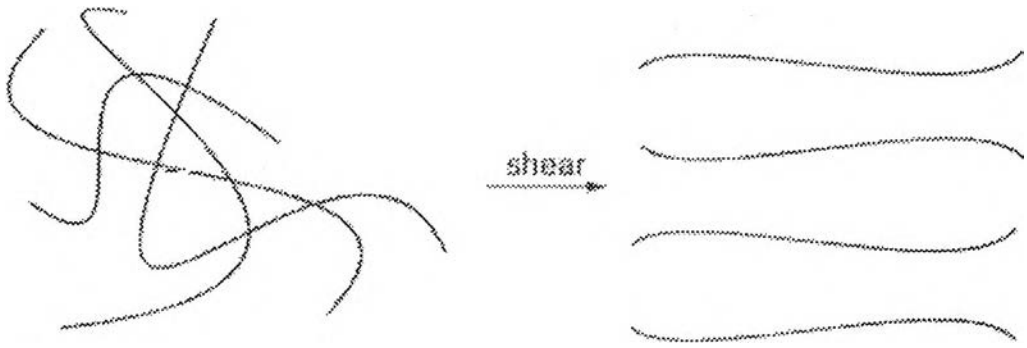

Figure 2.4 Idealized view of the effect of shear on the entanglement of concentrated polymer solutions and polymer melts.

In rare case, the viscosity may increase with increasing shear rate. Fluids that exhibit this behavior are called shear-thickening (or dilatant). Examples of shear-thickening behavior are generally limited to concentrated suspensions such as PVC pastes and polymer melts that undergo shear-induced crystallization.

2.4.1.2 Molecular Weight Dependence

The significance of entanglement to shear-thinning flow suggests that molecular weight and the critical molecular weight for entanglements, M_c, should significantly influence the rheological properties of polymers. It has been shown that the zero-shear viscosity, η_o, is directly related to the weight-average molecular weight, $\overline{M}_w$, when $\overline{M}_w < M_c$, but follows a 3.4 power dependence on $\overline{M}_w$ when $\overline{M}_w \geq M_c$. In addition, the onset of shear-thinning behavior occurs at progressively lower $\dot{\gamma}$ as molecular weight increases, as shown by viscosity data for polystyrene given in Figure 2.5.

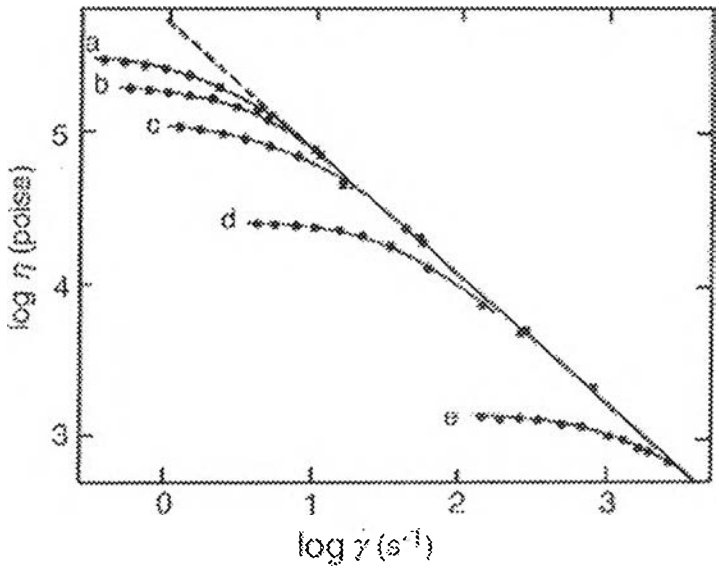

Figure 2.5 Effect of increasing molecular weight on the dependence of polymer viscosity on $\dot{\gamma}$ for polystyrene (Mc = 31,200) at 183°C. Molecular weights are (a) 242,000; (b) 217,000; (c) 179,000; (d) 117,000 and (e) 48,500.

2.4.1.3 Temperature Dependence

The temperature dependence of the apparent viscosity of the polymer melts follows a typical *Arrhenius relationship* at high temperatures, ca. 100°C above T_g, as given by

$$\eta = \eta_r \exp\left[\frac{E}{R}\left(\frac{1}{T} - \frac{1}{T_r}\right)\right] \qquad (2.4)$$

where η_r is the viscosity at some reference temperature, T_r, E is the activation energy (typically 21 to 210 kJ mol^{-1}), and R is the ideal gas constant. At lower temperatures, in the vicinity of glass-transition temperature, approximately $T_g < T < T_g + 100°C$, viscosity increases much more rapidly with decreasing temperature than given by the Arrhenius expression. In this case, the temperature dependence of melt viscosity can be obtained by the Williams-Landel-Ferry (WLF) equation as

$$\log\left[\frac{\eta(T)}{\eta(T_g)}\right] = \log a_T = \frac{-C_1(T - T_g)}{C_2 + T - T_g} \tag{2.5}$$

wherer $\eta(T_g)$ is the viscosity at T_g. Figure 2.6 shows the fit of experimental data for polycarbonate, for which excellent agreement between experimental viscosities and those predicted by the WLF equation is observed over the temperature range from T_g + 55°C to T_g + 185°C.

One view of the glass transition is that it is an isoviscose state where the viscosity at T_g, $\eta(T_g)$, is approximately 10^{12} Pa-s (10^{13} poise). Use of eq. 2.5 provides a means of relating the WLF parameters, C_1, and C_2, to the free volume, V_f, and the thermal-expansion coefficient, α, of the polymers.

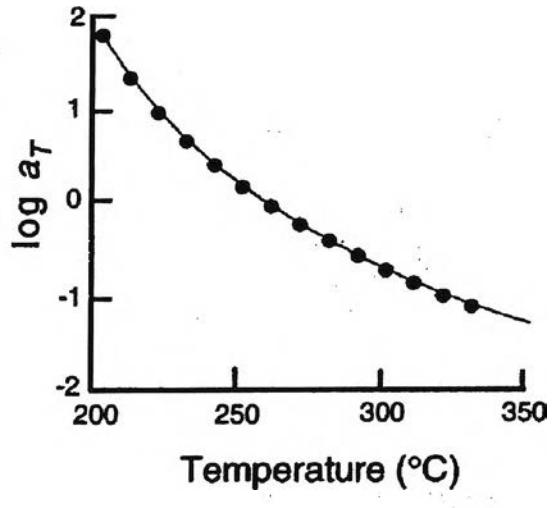

Figure 2.6 WLF fit (curve) of the shift factor, $a_T = \eta(T)/\eta(260°C)$, for polycarbonate at a reference temperature of 260 °C.

2.4.1.4 Pressure Dependence

Unlike the case for glass-transition temperature, viscosity can be significantly affected by pressure. This pressure dependence may be an important consideration in the design of some processing operations, such as injection molding for which pressure of several thousand psi are routinely experienced. At constant temperature, the effect of pressure on viscosity can be approximated by the relation

$$\ln\left(\frac{\eta}{\eta_r}\right) = \beta(p - p_r) \tag{2.6}$$

where η_r is a reference viscosity corresponding to some reference pressure, p_r, and β is a pressure coefficient in the range of 0.87 to 4.93 × 10^{-8} Pa^{-1} (0.6 to 3.4 × 10^{-4} $psia^{-1}$). As an example, the viscosity of a polystyrene melt at 250°C will nearly double with an increase in pressure from 13.8 to 27.6 MPa (2000 to 4000 psi). Often, in the modeling of processing operations, it is necessary to neglect the effect of pressure in order to obtain analytical or even numerical solutions that are manageable.

2.4.1.5 Time Dependence

Shear-thinning (and shear-thickening) behavior is considered to be reversible providing no thermal or mechanical degradation has occurred. In some cases, the subsequent flow behavior of a previously sheared fluid may depend upon the prior shear history and time allowed for recovery. A fluid whose viscosity is reduced by prior deformation or decreases with time under conditions of constant shear stress or shear rate is called thixotropic. Eventually, the viscosity will recover (increase) once the stress is removed. An example of a thixotropic fluid is nondrip latex paint. Similarly, a fluid whose viscosity has increased as a result of prior deformation history or increases in time under application of constant stress or strain is called antithixotropic. As will be shown shortly, the successful modeling of polymer processing operations is difficult enough without introducing time-dependent viscosity terms, and no attempt to do so will be made here.

2.4.2 Viscosity of Polymer Solution and Suspension

2.4.2.1 Solution Viscosity

For very dilute solutions, polymer coils are widely separated and do not overlap, as illustrated in Figure 2.7. At a critical concentration, c^{**}, making the transition from the extremely dilute to diute regions, the hydrodynamic volumes of individual coils start to touch. As concentration is further increased ($c > c^*$), colis begin to overlap and finally entanglements are formed that increase viscosity.

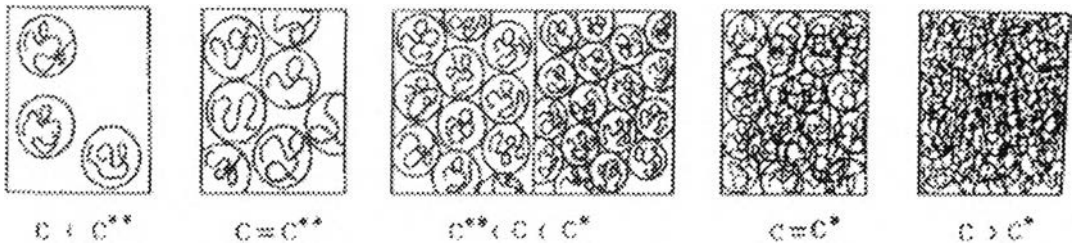

Figure 2.7 Critical concentration regions showing transition from the extremely dilute regions ($c < c^{**}$) where polymer coils are isolated to the dilute region ($c > c^*$) where coils become entangled.

The critical concentration, c^*, may be marked by an abrupt increase in the relative viscosity increment (or specific viscosity). This transition is shown for cellulose acetate (CA) in dimethyl sulfoxide (DMSO) in Figure 2.8. The critical transition concentration was found to be 3.7 g dL^{-1} and approximately independent of the solvent, although a dependence of c^* on the molecular weight of CA would be expected.

Below c^*, viscosity is proportional to concentration, but above c^*, viscosity is approximately proportional to the fifth power of concentration. In general, the effect of molecular weight and solution concentration of viscosity can be modeled as

$$\eta = K(cp)^{\alpha} M^{\beta} \qquad (2.7)$$

where K is constant and α and β are parameters; the ratio β/α is usally in the range from 0.54 to 0.74.

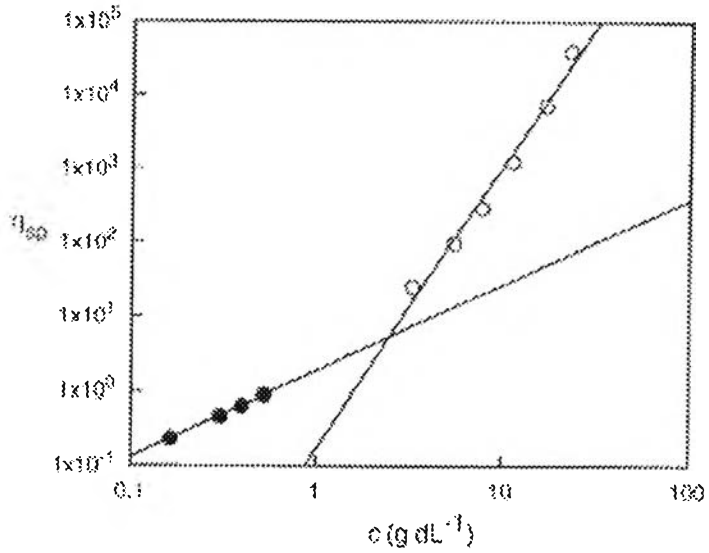

Figure 2.8 Concentration dependence of the specific viscosity of dilute and moderately concentrated solutions of cellulose acetate in dimethyl sulfoxide. The intersection of straight line that are drawn through the dilute-solution (•) and concentrated-solution (○) data marks the critical concentration, c^* (ca. 3.7 g dL^{-1} in this case).

The presence of a solvent (or plasticizer) has two effects on polymer viscosity in the concentrated solution regions: the solvent (1) lowers the T_g and (2) increases the molecular weight between entanglements, M_e, as

$$M_e = \frac{M_e^o}{\phi} \tag{2.8}$$

where M_e^o is the molecular weight between entanglements for the undiluted polymer and ϕ is the volume fraction of the solvent. As polymer concentration increases, polymer solutions become more non-Newtonian as the number of entanglements increases, as illustrated for concentrated solutions of polystyrene in n-butyl benzene in Figure 2.9. The data show that viscosity of a concentrated polymer solution rapidly increases with increasing polymer concentration. In addition, the onset of shear-thinning behavior occurs at lower shear rate with increasing concentration.

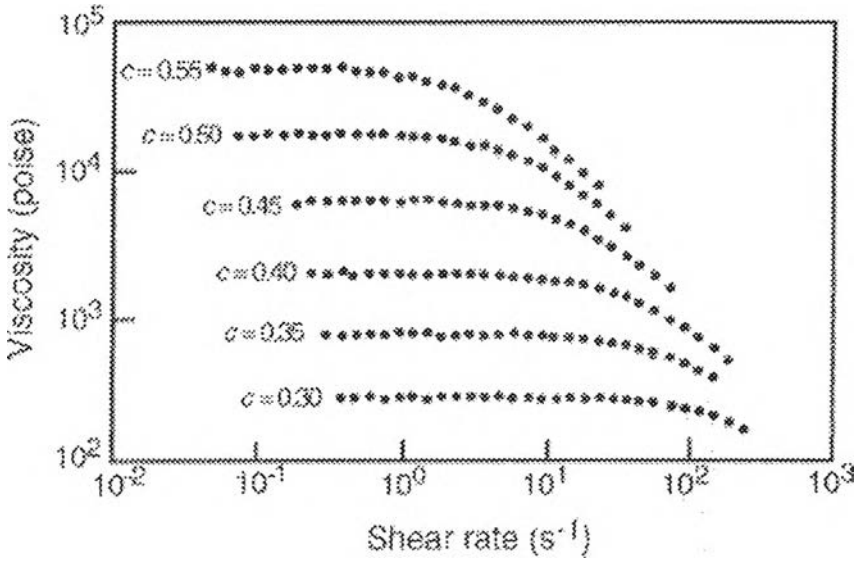

Figure 2.9 Viscosity of polystyrene (411,000 molecular weight) in *n*-butyl benzene at different concentration (c, unit of g cm^{-1}) as a function of shear strain-rate ($\dot{\gamma}$) at 30°C.

2.4.2.2 Viscosity of Suspensions

In many cases, concentrated polymer solutions and melts may contain particulate or fiber fillers. For example, commercial rubber formulations usually contain carbon black. Poly(vinyl chloride) for floor tile or wire insulation applications typically contains rigid fillers such as calcium carbonate. A plastisol is a suspension of polymer particles in a liquid plasticizer, while a latex is a suspension of particles in water. In all these cases, suspended particles affect the rheological properties of the suspension.

In 1960, Einstein theorized that the viscosity of dilute suspensions in a Newtonian liquid can be expressed as

$$\eta = \eta^{o}(1 + k_{E}\phi) \tag{2.9}$$

where η^{o} is the viscosity of the suspending liquid, k_E is called the Einstein coefficient, and ϕ is the volume fraction of suspended particles. The Einstein coefficient depends upon the geometry of the dispersed phase as well as the orientation of fibers and other nonspherical fillers. In the case of spherical fillers, such as calcium carbonate, k_E, is 2.5. Equation 2.9 indicates that the relative viscosity, η/η^{o}, depends only upon the concentration of filler and is independent of the size and nature

of the particles. Over the years, many other equations have been proposed with various degree of success. One of the best was proposed by Mooney, given as

$$\ln(\eta/\eta^{o}) = \frac{k_E \phi}{1 - \phi/\phi_m} \tag{2.10}$$

where ϕ_m is the maximum packing (volume) fraction, which varies from 0.065 for rod-shaped particles to 0.7405 for hexagonal close-packed spheres. It may be noted that even Newtonian fluids such as water become non-Newtonian at moderate concentrations of suspended particles. Some suspensions such as lattices and plastisols exhibit yield (Bringham) behavior, as the following section.

2.4.3 Constitutive Equations

In order to model a simple-flow geometry as a prelude to handling more complicated processes such as extrusion, it is necessary to begin with some reasonable model for the relation between shear stress and shear rate (eq. 2.3). the most widely used relationship is the power-law (or Ostwald-de Waele-Nutting) model given as

$$\tau = m\dot{\gamma}^{n} \tag{2.11}$$

where m is called the consistency and n is the *power-law* index. For a given polymer, m is decreasing function while n is an increasing function of increasing temperature, which means that the melt become Newtonian (i.e., less shear thinning) with an increase in temperature. It follows from the GNF model given by eq. 2.3 that the dependence of apparent viscosity, η, on $\dot{\gamma}$ for a power-law fluid (PLF) is

$$\eta = m\dot{\gamma}^{n-1}. \tag{2.12}$$

Equation 2.12 indicates that, when $n = 1$, η is independent of $\dot{\gamma}$. This mean that Newtonian's law of viscosity may be considered to be a special case (i.e., $n = 1$ and $m = \mu$) of the more general PLF model. For shear-thinning behavior, $n < 1$. Representative values of the power-law parameters, m and n, and the $\dot{\gamma}$ range for which they are applicable are given for several commercially important polymers in Table 2.1.

Some non-Newtonian fluids require an application of the threshold (or yield) stress, τ_y, before flow will begin. Such fluids are termed Bingham fluids and

may be viewed as having some internal structure that collapses at τ_y. Examples include some suspensions, slurries, pulps and ketchup. If the viscous response is Newtonian once the yield stress has been reached, the constitutive equation for a Bingham fluid can be written as

$$\tau = \tau_y + \mu\dot{\gamma}. \tag{2.13}$$

It is clear that equation 2.12 is suitable for representing the dependence of viscosity on shear rate only in the shear-thinning region where a plot of log η versus log $\dot{\gamma}$ is linear. Since this is normally the $\dot{\gamma}$ range for most important processing operations, particularly extrusion and injection molding (see Table 2.2), this restriction is seldom significant considering the simplicity of the model. Other constitutive equations, such as the Carreau model, are available to fit data over a more extensive $\dot{\gamma}$ range but typically, make the solution to processing problems more difficult.

Table 2.1 Power-law parameters for some representative polymers

Polymer	Temperature (°C)	$\dot{\gamma}$ Range (s^{-1})	m $N\ s^n m^{-2}$	N
Polystyrene	190	100-4500	4.47×10^4	0.22
	210	100-4500	2.38×10^4	0.25
	225	100-5000	1.56×10^4	0.28
Polypropylene	180	100-400	6.79×10^3	0.37
	190	100-3500	4.89×10^3	0.41
	200	100-4000	4.35×10^3	0.41
Polycarbonate	180	100-1000	8.39×10^3	0.64
	200	100-1000	4.31×10^3	0.67
	220	100-1000	1.08×10^3	0.80

Table 2.2 Typical $\dot{\gamma}$ range for polymer processing operations

Operation	$\dot{\gamma}$ Range (s^{-1})
Compression molding	1-10
Calendaring	$10\text{-}10^2$
Extrusion	$10^2\text{-}10^3$
Injection molding	$10^3\text{-}10^4$